

PRELIMINARY STUDY OF ADVANCED LLRF CONTROLS AT LANSCE FOR BEAM LOADING COMPENSATION IN THE MaRIE X-FEL *

A. Scheinker[†], M. Prokop, J. Bradley III, P. Torrez, L. Castellano, S. Kwon, D. Knapp, J. Lyles, S. Baily, J. Hill, D. Rees, Los Alamos National Laboratory, Los Alamos, USA

Abstract

The analog low level RF (LLRF) control system of the Los Alamos Neutron Science Center is being upgraded to a Field Programmable Gate Array (FPGA)-based digital system (DLLRF). In this paper we give an overview of the FPGA design and the overall DLLRF system. We also present preliminary performance measurements including results utilizing model-independent iterative feedforward for beam-loading transient minimization, which is being studied for utilization in the future MaRIE X-FEL [1], which will face difficult beam loading conditions.

INTRODUCTION

A digital low level RF (DLLRF) system upgrade has been in development at the Los Alamos Neutron Science Center (LANSCE) proton linear accelerator for many years [2], to replace the existing analog feedback control system. Although the simple analog system has performed reliably over the years, the move towards a digital control system was inspired by many factors including the possibilities of: remote control tuning via ethernet, the ability to quickly switch between controller setups for various beam types, and to implement iterative updates to controller outputs in-hardware to implement exotic adaptive control algorithms (during the ~ 8 milliseconds between RF pulses, as demonstrated in this work). This transition is made possible by the availability of affordable, fast (> 100 MS/s), high resolution (16 bit) analog to digital converters (ADC) and fast (~ 125 MHz) field programmable gate arrays (FPGA).

The ability to switch between multiple controllers between beam pulses is especially important for LANSCE where a large variety of beam types, each of which has its own influence on the RF cavity fields via various levels of beam loading. The LANSCE experimental facilities include: 1) The Lujan Center, which requires short high intensity proton bunches in order to create short bursts of moderated neutrons with energies in the meV to keV range. 2) The Proton Radiography (pRad) Facility, which provides movies of dynamic phenomena in bulk material (for example, shock wave propagation) via 50 ns proton bursts, repeated as frequently as 358 ns with programmable burst repetition intervals. 3) The Weapons Neutron Research (WNR) Facility, which provides unmoderated neutrons with energies in the keV to MeV range. 4) The Isotope Production Facility (IPF), which produces medical radioisotopes for US hospitals. 5). The Ultra Cold Neutrons (UCN) Facility, which creates neutrons with en-

ergies below μeV for basic physics research. The various beam flavors at LANSCE are summarized in Table 1.

Table 1: Parameters of LANSCE 625 μs Pulse Width Beams at 800 MeV, H^- , and 100 MeV, H^+ (IPF)

Beam	Ave Current [μA]	Rep Rate [Hz]	Ave Power [kW]
Lujan	100 – 125	20	80 – 100
pRad	< 21	~ 1	< 1
WNR	< 2	100	~ 3.2
UCN	< 5	20	< 4
IPF	460	100	46

The ability to handle various beam loading conditions, some of which are extreme, will also be crucial for the Matter-Radiation Interactions in Extremes (MaRIE) X-FEL linac currently being designed [1].

MaRIE X-FEL LLRF REQUIREMENTS

The MaRIE X-FEL linac will accelerate electrons up to 12 GeV via superconducting (SC) 1.3 GHz TESLA-type cavities, with the goal of producing 42 keV X-rays with electron bunches of 8 mA average current over macropulse lengths of 69 ns – 700 μs . The MaRIE linac will also produce short, intense pulses for electron radiography (eRad). The spacing of electron bunches will be customizable. Typical X-Ray FEL bunches will be 0.2 nC. The average current will be 8 mA over the entire macropulse, with drastically decreasing bunch spacing, down to 2.3 ns, for the final 230 ns of the pulse. The eRad experiments will require 2 nC micropulses which will be interleaved within the same macropulse as the X-ray FEL bunches, with a separation of 24 ns after individual eRad micropulses. The extreme beam loading caused by closely spaced high current bunches will require the use of much faster (lower Q) normal conducting cavities to make up for the energy droop introduced in the SC sections, whose extremely high Qs would require prohibitively large klystron power inputs for beam loading compensation [3, 4].

DIGITAL LLRF OVERVIEW

Signal Processing

The cavity and master oscillator (MO) RF signals, both at a frequency $f_{\text{RF}} = 201.25$ MHz, are sampled via standard IQ sampling. First the signals are down-converted to $f_{\text{IF}} = 25$ MHz by mixing with a local oscillator (LO) signal at

* Work supported by Los Alamos National Laboratory

[†] ascheink@lanl.gov

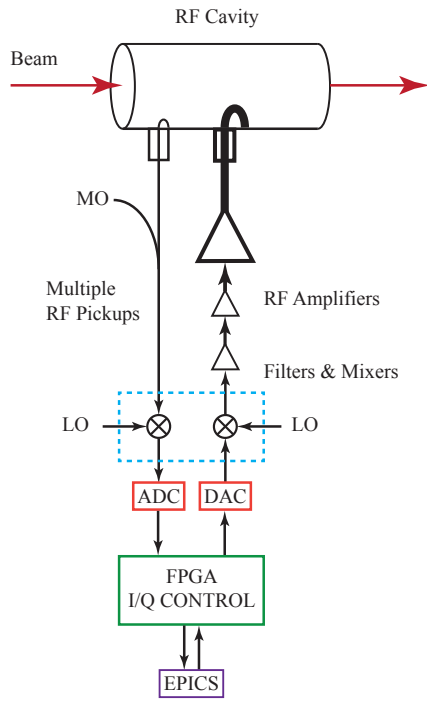


Figure 1: Digital low level RF setup.

$f_{LO} = 176.25$ MHz, resulting in IF signals of the form

$$\begin{aligned} V_{cav}(t) &= A_{cav}(t) \cos(2\pi f_{IF}t + \theta_{cav}(t)) \\ &= \underbrace{A_{cav}(t) \cos(\theta_{cav}(t))}_{I_{cav}(t)} \cos(2\pi f_{IF}t) \\ &\quad - \underbrace{A_{cav}(t) \sin(\theta_{cav}(t))}_{Q_{cav}(t)} \sin(2\pi f_{IF}t), \end{aligned}$$

which is then sampled at a rate $f_s = 4 \times f_{IF} = 100$ MHz, resulting in the FPGA collecting ADC I and Q samples directly at time steps $nt_s = \frac{n}{f_s}$:

$$\{I_{cav}(0), -Q_{cav}(t_s), -I_{cav}(2t_s), Q_{cav}(3t_s), \dots\},$$

which are then cleaned up with a moving average filter. The MO signal is sampled in the same way, and the phase of the MO signal and its sine and cosine are then retrieved utilizing a CORDIC algorithm. Finally, the cavity signal is phase shifted relative to the master oscillator to calculate I and Q measurements of the cavity relative to the reference (see Fig. 1).

Standard Control Method

Once the I and Q signals are detected, they are compared to set points and the errors, I_e and Q_e , are fed into a proportional-integral (PI) feedback controller whose outputs are given by

$$\begin{aligned} u_I(t) &= -k_p I_e(t) - k_i \int_0^t I_e(\tau) d\tau, \\ u_Q(t) &= -k_p Q_e(t) - k_i \int_0^t Q_e(\tau) d\tau. \end{aligned}$$

The PI feedback system's gains are limited by delays, which place upper bounds on control gains which can be used without destabilizing the system, which limits the system's

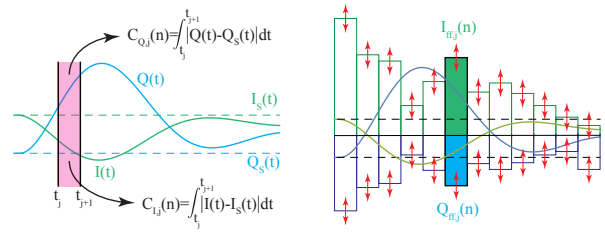


Figure 2: **Left:** Iterative scheme for determining I and Q costs during 1–10 μ s intervals. **Right:** ES-based feedforward outputs for beam loading transient compensation.

ability to respond to fast transients, such as those caused by beam loading. Therefore, in addition to PI-based feedback, we utilize a static feed-forward signal, which is based on a measurement of the beam current at the entrance of the accelerator, a signal which then outruns the slow protons and is fed as a feed-forward into the controller outputs to compensate for beam loading. For MaRIE, where the electron beam travels at $v \sim c$, a scheduled rather than measured beam current profile would have to be used.

The static feedforward improves controller performance, but its success faces limitations due to a limited resolution and imperfect measurement of the beam current signal which is being fed back into the system in order to mitigate beam loading effects based on an assumed form of a linear time invariant system. The success of this approach is further limited by several factors, including: 1) Time-varying uncertainty in the system. 2) A linear approximation as a system model. 3) The beam impulse excites many higher order modes and the dynamics of all of the various cavity modes are coupled together. In order to improve performance beyond what is possible using PI and static feedforward alone, we implemented an iterative extremum seeking (ES) feed forward method as described below.

Advanced Control Method Development

The ES controller is a model-independent method for stabilizing and optimizing unknown, many parameter, noisy systems, able to tune many parameters simultaneously based only on a scalar noise-corrupted cost function [5–7] which has been utilized in software and in hardware for automated particle accelerator tuning [8, 9]. For ES, the detected RF signal was broken down into 10 ns – 10 μ s long sections and feed forward $I_{ff,j}(n)$ and $Q_{ff,j}(n)$ control outputs were generated for each section, as shown in Figure 2.

The iterative extremum seeking was performed by updating the feedforward signals according to

$$\begin{aligned} I_{ff,j}(n+1) &= I_{ff,j}(n) + \Delta\sqrt{\alpha\omega} \cos(\omega n\Delta + kC_{I,j}(n)) \\ Q_{ff,j}(n+1) &= Q_{ff,j}(n) + \Delta\sqrt{\alpha\omega} \sin(\omega n\Delta + kC_{Q,j}(n)) \end{aligned}$$

where the individual I and Q costs were calculated as

$$C_{I,j}(n) = \int_{t_j}^{t_{j+1}} |I_e(t)| dt, \quad C_{Q,j}(n) = \int_{t_j}^{t_{j+1}} |Q_e(t)| dt.$$

EXPERIMENTAL RESULTS

The experimental results are shown in Figure 3 and summarized in Table 2, for iterative sections of length $10\ \mu\text{s}$. The maximum, rms, and average values are all calculated during a $150\ \mu\text{s}$ window which includes the beam turn on transient to capture the worst case scenario. The ES-based scheme is a $> 2\times$ improvement over static feed-forward in terms of maximum errors and a $> 3\times$ improvement in terms of rms error.

Table 2: DLLRF Performance During Beam Turn on Transient

	No Beam	Beam, No ES	Beam & ES
max A error (%)	± 0.06	± 0.41	± 0.22
rms A error (%)	0.025	0.168	0.066
mean A error (%)	-0.003	-0.114	-0.024
max θ error (deg)	± 0.09	± 0.57	± 0.21
rms θ error (deg)	0.028	0.283	0.108
mean θ error (deg)	0.016	-0.208	-0.034

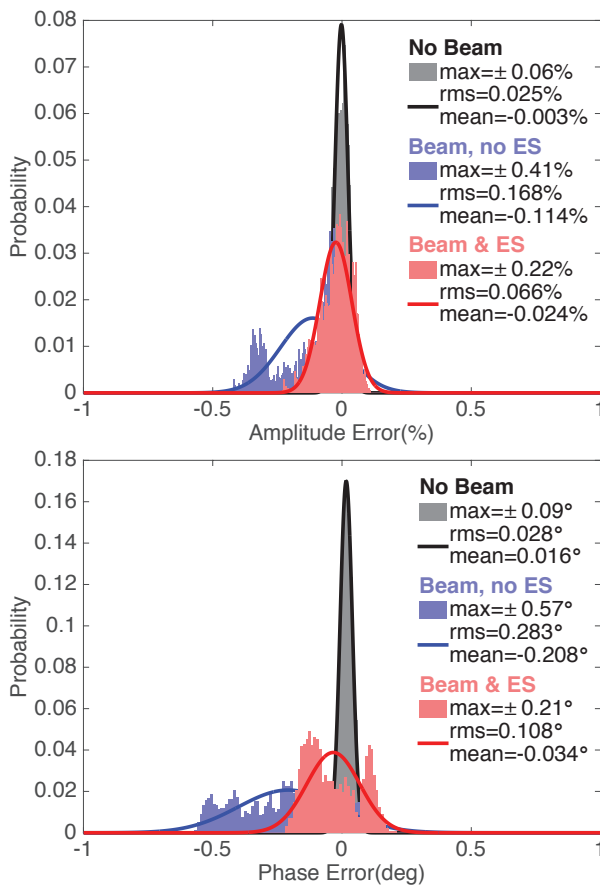


Figure 3: Phase and amplitude errors shown for $150\ \mu\text{s}$ long data bin that spans the time before, during, and after beam turn-on transient. The data shown is cleaned up via 100 point moving average of raw data which was sampled at 100 MS/s.

CONCLUSIONS

The results presented here are preliminary but already show a well functioning DLLRF system. The ES algorithm has just been implemented and we have only had a few days of beam time for its development. We expect the beam transient to be almost un-detectable once the ES algorithm is properly set up and tuned.

Furthermore, the results shown here are based on iterative ES using $10\ \mu\text{s}$ long windows for feed forward. Performance improvements have already been seen with smaller windows, down to $1\ \mu\text{s}$, with the high speed FPGA utilizing built in RAM to easily perform all calculations and feed forward updates in-hardware between beam pulses ($< 8\text{ms}$).

We plan on testing the algorithm with windows down to the 10 ns length, as is possible with the Stratix III FPGA being used. For MaRIE applications, for bunch separation of $\sim 10\ \text{ns}$, we will utilize faster FPGAs, allowing for individual feed forward windows down to several ns.

REFERENCES

- [1] J. Bradley III, D. Rees, A. Scheinker, and R. L. Sheffield, "An Overview of the MaRIE X-FEL and Electron Radiography LINAC RF Systems," in *Proc. IPAC'15*, Richmond, Virginia, USA, 2015.
- [2] J. Lyles, W. Barkley, Jerry Lee Davis, Angela Carol Naranjo, Mark S. Prokop, Daniel Earl Rees, and M. Gilbert Jr *et al.*, "Results from the Installation of a New 201 MHz RF System at LANSCE," in *Proc. LINAC'14*, Geneva, Switzerland, 2014.
- [3] R. L. Sheffield, "Enabling cost-effective high-current burst-mode operation in superconducting accelerators," *Nuclear Instruments and Methods in Physics Research Section A: Accelerators, Spectrometers, Detectors and Associated Equipment* 785, pp.197-200, 2015.
- [4] J. Bradley III, A. Scheinker, D. Rees, and R. L. Sheffield, "High power RF requirements for driving discontinuous bunch trains in the MaRIE linac," presented at the LINAC Conference, East Lansing, MI, USA, 2016.
- [5] A. Scheinker and M. Krstic, "Maximum-seeking for CLFs: Universal semiglobally stabilizing feedback under unknown control directions," *IEEE Transactions on Automatic Control*, vol. 58, pp. 1107-1122, 2013.
- [6] A. Scheinker and M. Krstic, "Extremum seeking with bounded update rates," *Systems & Control Letters*, vol. 63, pp. 25-31, 2014.
- [7] A. Scheinker and D. Scheinker, "Bounded extremum seeking with discontinuous dithers," *Automatica*, vol. 69, pp. 250-257, 2016.
- [8] A. Scheinker, X. Pang, and L. Rybarczyk. "Model-independent particle accelerator tuning," *Physical Review Special Topics-Accelerators and Beams*, 16.10, 102803, 2013.
- [9] A. Scheinker and S. Gessner, "Adaptive method for electron bunch profile prediction." *Physical Review Special Topics-Accelerators and Beams*, 18.10, 102801, 2015.